Analysis of saturation signal correction of the troposphere lidar

Zhishen Liu (刘智深)*, Zhigang Li (李志刚), Bingyi Liu (刘秉义), and Rongzhong Li (李荣忠)

Key Laboratory of Ocean Remote Sensing, Ministry of Education of China, Ocean University of China, Qingdao 266003, China

**E-mail: zsliu@orsi.ouc.edu.cn*

Received January 14, 2009

Usually, lidar detection systems are optimized for the measurement of the low intensity signal using the photon counting technique, but this approach results in the nonlinear signal response for the higher intensity signal. The problem is successfully solved by the combination of analog-to-digital (AD) and photon-counting (PC) detection. The optimized processing procedure of the signal combination of AD and PC is described, and the corrected result is analyzed and compared with the results by the dead-time correction method. In this way, the accuracy of wind and aerosol measurement in the nonlinear range is improved. In addition, the signal-to-noise ratios (SNRs) of the two detection methods of AD and PC are compared in the overall dynamic range of signal for the performance analysis.

OCIS codes: 280.3640, 030.5260.
doi: 10.3788/COL20090711.1051.

Most lidar systems for the low or middle layer atmosphere measurements adopt photon-counting (PC) mode because of the high detection sensitivity, resolution, and stability. However, PC mode can only be used for detecting weak and ultra weak light. For the troposphere detection, the signal dynamic range of lidar is very large and the electron pulses from photomultiplier tube (PMT) in low altitude are too closely spaced in time to be discriminated by the photon-counter, which is called as pulses pile-up. The effect of pile-up will cause the observed counting rate to be nonlinear with respect to the true counting rate. This effect can be reduced by using quick-response PMT and suited output circuit, or high resolution photon-counter. Besides, a careful choice of the discriminator threshold is critical in maximizing the linear operating range of PC system, and it has been demonstrated by Darland *et al.*[1] and Donovan *et al.*[2]

The dead-time correction can be used for the saturation correction to extend the dynamic range[3−5], but the correction error is unavoidable due to the uncertainty of hardware specifications. The method based on the combination of analog-to-digital (AD) and PC data can be well used to extend the signal dynamic range for the troposphere detection. A Doppler wind lidar based on the iodine filter was developed for the tropospheric wind measurement by Liu *et al.*[6−8] The edge technique was used for the Doppler discrimination. In addition, the backscattering ratio $R_{\rm b}$ can be calculated by the successful separation of aerosol and molecular backscattering signals[6]. The lidar system encounters a wide dynamic range, with a detection range up to 10 km. The objective of the use of parallel AD and PC detection is to extend the dynamic range.

PC electronics have a minimum pulses resolving time τ known as the dead time. The capability of the photon counter is limited partly by the maximum counting rate due to the assumption of the pulse train and the Possion statistics of the lidar signals. The photon counters are broadly classified into two types, paralyzable and nonparalyzable counters distinguished by the counter behavior. A paralyzable counter is unable to provide a second counting unless there is a resolving time τ between two successive input pulses, and the dead time will extend to the next pulse if this pulse arrives during its resolving time[9]. The response of a paralyzable counter will tend to zero if the true counting rate is large enough. The photon correction equation to the paralyzable counter is nonlinear and can be expressed as

$$N_{\rm obs} = N_{\rm true}\exp(\tau N_{\rm true}), \tag{1}$$

where $N_{\rm obs}$ is the observed counting rate and $N_{\rm true}$ is the true counting rate.

A nonparalyzable counter is one whose dead time will not extend to the next pulse if this pulse arrives during its resolving time. The counting rate will asymptotically tend toward a maximum observed counting rate as the increase of the true counting rate[9]. The observed counting rate is expressed as:

$$N_{\rm obs} = \frac{N_{\rm true}}{1+\tau N_{\rm true}}. \tag{2}$$

Equations (1) and (2) are only theoretical models. It is clear that the dead time correction for the nonparalyzable counter is invalid when $N_{\rm obs}$ is equal to the maximum counting rate. The true photon counting rate is traditionally regarded as being located at somewhere between the two behaviors. Since the photon counter in our lidar system shows the dominant characteristics of a nonparalyzable behavior, the dead time correction method of Eq. (2) is used.

For the wind lidar, the Licel transient recorder systems have a parallel AD and PC detection chain, with the integration of both detection mechanisms into a single device. The output AD signal is comparable to the signal fed into the AD converter. As the effect of pile-up increases, the

AD signal will increase proportionally; however, PC will cause a nonlinear signal due to the disability to distinguish the pulses. For high counting rates, the linearity of the AD signal is superior to the PC signal, which is the reason to extend the detection dynamic range by the combining use of AD and PC.

For the saturation signal, the true photon counting rate can be seen as the equivalent one calculated from AD signal because of its high dynamic range. The relation between the voltage of AD and $N_{\rm true}$ is only related to the gain coefficient G of PMT, resistance R, and sampling time t. Then the relation between AD and PC signals should be linear due to the constant values of G, R, and t, where good signal-to-noise ratio (SNR) of AD and nonsaturation of PC are obtained.

The main idea of the signal combination is that there is a region where both signals are valid and have a high SNR. The first fraction of the combination known as "gluing" is to find a region of the signal where both of AD and PC can be regarded as linear ones. A typical region of 1−20 MHz was normally used for the application due to the linear response and preferable SNR to AD signal[10]. The background signal should be subtracted firstly for both of the AD and PC signal. The combining algorithm is described as the minimal bias by the calculation of a and b:

$$\sum_{N_{\rm PC}=1\ {\rm MHz}}^{20\ {\rm MHz}} \{N_{\rm PC}(n) - [aV_{\rm AD}(n) + b]\}^2 = {\rm minimum}, \quad (3)$$

where $N_{\rm PC}$ (n) and $V_{\rm AD}$ (n) are the photon counting rate and signal voltage at the range gate of n, respectively, which are measured by the device with the combination of AD and PC detection, a and b are the slope and offset of the best-fit regression.

The observation data with 3 million pulses accumulation are used for the combination analysis of AD and PC in this letter. In order to decrease the influence from the signal fluctuation of the boundary layer or cloud return, the exceptional horizontal atmospheric detection is achieved by the hemispherical scanner. The dead time correction should be firstly used. Figure 1 shows the necessity of the application of dead-time correction. The nonparalyzable correction is done using 4-ns resolving time (corresponding to 250-MHz maximum counting rate). A distinct error to the best-fit regression in the region of higher counting rate can be seen for the situation without dead time correction, and there is a slope difference of ∼10% for the regressions.

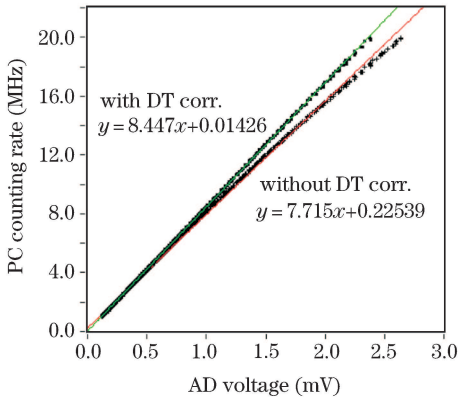

Fig. 1. Regressions of AD-PC data with and without dead time correction (DT corr.).

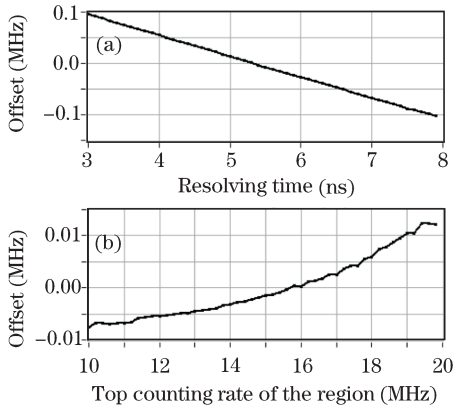

Fig. 2. Optimization of the resolving time and the linear response region by near zero-offset.

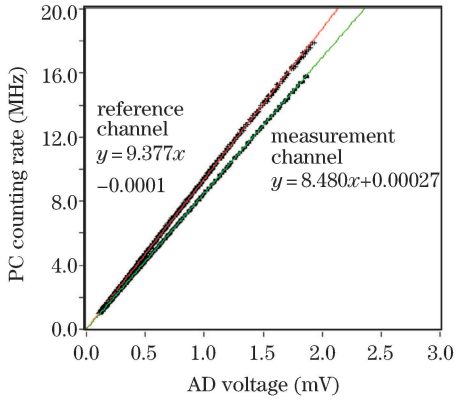

Fig. 3. Regressions of AD-PC data of measurement and reference channels.

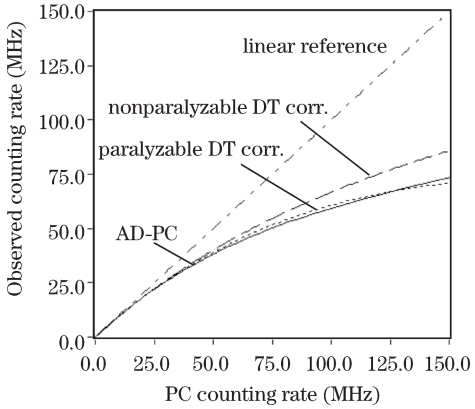

Fig. 4. Comparison of correction methods including two kinds of dead time correction and AD-PC combination.

The resolving time of the photon counter shows a bit difference to the value which is determined by the maximum counting rate, due to the influence from pulse width determined by detectors and the discriminator level of the photon counter. The real resolving time can be determined by empirical methods[11,12]. A method based on the zero-offset (value b) of the regression versus resolving time is used for the optimization[13]. The optimized

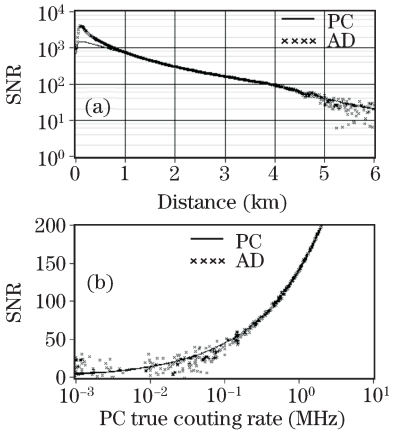

Fig. 5. SNR comparison for AD and PC detection.

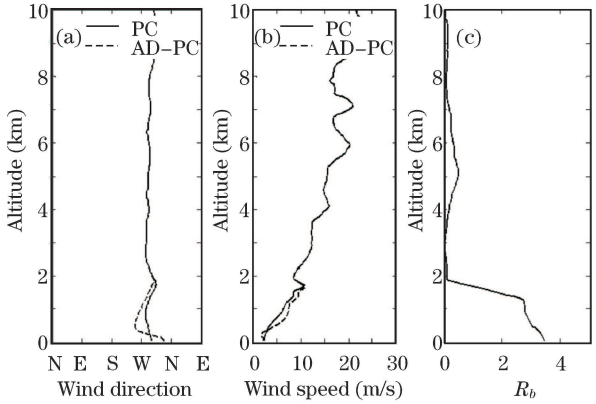

Fig. 6. Accuracy improvement for wind detection by AD-PC combination around 20:00 on 30 January 2007. (a) Wind direction and (b) wind speed profiles derived by PC data and AD-PC combination; (c) derived $R_{\rm b}$ profile.

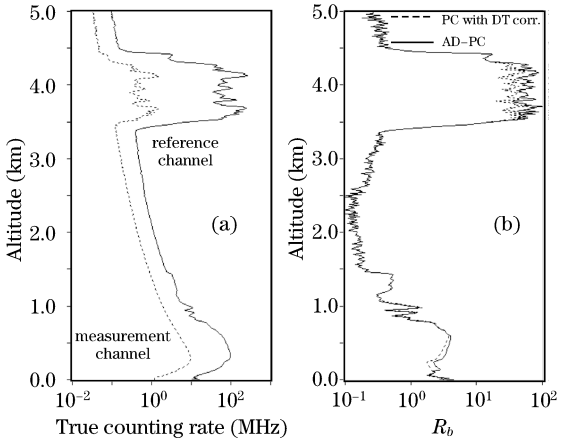

Fig. 7. Accuracy improvement for aerosol detection by AD-PC combination. (a) Lidar signals of both channels; (b) $R_{\rm b}$ profiles derived by PC data and AD-PC combination.

dead time of 5.3 ns produces a near zero-offset, and the dead time of 4 ns produces an offset error of ∼0.05-MHz. The analysis result is shown in Fig. 2(a). The difference of the selected region with linear response will produce the difference of the regressions. The optimizing method based on the zero-offset is also used for determining the top counting rate of the region. The result is shown in Fig. 2(b) with near zero-offset at 16 MHz. Then a region of 1−16 MHz is selected for the combination calculation.

The combination calculation should be done separately for both channels due to the performance difference between detectors and electronics. The combination regressions for the both channels are shown in Fig. 3. The optimized resolving time of 5.3 and 5.1 ns, the optimum linear regions of 1−16 and 1−18 MHz are used for the calculation, corresponding to the measurement channel and the reference channel. A slope difference of approximate 10% exists between the channels. Once the transfer coefficients of a and b are determined, they can be used for routinization instead of searching in every signal for new coefficients. The coefficients should stay constant if the PMTs have the same applied high voltage.

The true photon counting rate is calculated by transferring the nonsaturated AD signal to photon counting rate. The methods for saturation correction, including dead time correction of two behaviors and AC-PC combining correction, give a comparison, as shown in Fig. 4. All of them have good consistence below a low counting rate of 30 MHz; the dead time corrections only produce an incorrect correction for the high counting rate. The comparison indicates how different it is between the dead time corrected counting rate and the true one.

The benefit of AD-PC combination is the extension of the signal dynamic range. In addition, the signal analysis based on AD and PC synchronous detection is also available, and a good comparison can be done which was rarely discussed before. With the successful transformation from AD signal to PC signal, the photon counting rates for AD and PC detections are obtained, and then the SNR can be well used for the evaluation of the detection performance. The SNR is defined as

$$\mathrm{SNR} = \frac{N_s}{\sqrt{N_s + N_b + N_e}}, \tag{4}$$

where N_s is the laser backscattering signal, N_b is the noise produced by photons from the sky background, and N_e is the noise from the dark current. The SNR comparison of AD and PC detection is shown in Fig. 5. An increase with a factor of 4 for dynamic range is achieved in low altitudes. The comparison indicates a good consistency in the middle area when the SNR is larger than 100, and the PC represents a perfect advantage for the upper atmosphere detection with low intensity. Figure 5(b) shows the SNR corresponding to the true photon counting rate. The AD detection loses its capacity when the counting rate is less than ∼0.1 MHz.

The use of AD-PC combination will improve the accuracy of wind detection in the regions with saturated signal. Figure 6 shows the wind profile comparison derived from the PC data and AD-PC combination one, where the PC data are obtained after a nonparalyable dead time correction. As expected, the incorrect correction in low altitudes makes a great influence. It is indicated that the bias can go up to 3−4 m/s for wind speed and 45° for wind direction. We can explain that the high density aerosol in the boundary layer does a big contribution to the causation of the strong signal from the result of the aerosol backscattering ratio in that day.

The AD-PC combination is also useful for the results

improvement of the aerosol backscattering ratio R_b, especially for cloud detection. Figure 7(a) shows the lidar signals of two channels under cloudy weather condition. Figure 7(b) shows the calculated R_b profile. Two situations are considered, that is, the result derived by PC data with dead time correction and the result derived by AD-PC combination. The R_b derived by AD-PC combination increases by about 50% for the cloud at an altitude around 4 km, as well as an increase of around 20% in the boundary layer.

In conclusion, the saturation correction with the observations of troposphere wind lidar is analyzed. The combination of AD and PC detection signals is optimized with the determination of resolving time and linear region of the counting rate by the zero crossing for offset, and the true counting rate calculated by AD-PC combination is compared with the one corrected by the traditional dead time correction. The SNR of the AD and PC synchronous detection is analyzed under the same situation in the overall dynamic range of lidar signal. An increase with a factor of 4 for dynamic range is achieved. The AD detection performs linearly when the photon counting rate is larger than 0.1 MHz. The usefulness of the AD-PC combination has been made clear by the accuracy improvement of wind profiles and R_b value in troposphere detection.

This work is a part of the open project of the retrieval method of wind field from Doppler lidar which is financed by the Key Laboratory of Ocean Remote Sensing, Ministry of Education of China. This work was supported by the National Natural Science Foundation of China under Grant Nos. 60578038 and 40427001.

References

1. E. J. Darland, G. E. Leroi, and C. G. Enke, Anal. Chem. **51,** 240 (1979).
2. D. P. Donovan, J. A. Whiteway, and A. I. Carswell, Appl. Opt. **32,** 6742 (1993).
3. K. Omote, Nucl. Instrum. Methods Phys. Res. A **293,** 582 (1990).
4. M. Ware, A. Migdall, J. C. Bienfang, and S. V. Polyakov, J. Mod. Opt. **54,** 361 (2006).
5. J. W. E. van Dijk and H. W. Julius, Radiation Protection Dosimetry **84,** 359 (1999).
6. Z.-S. Liu, D. Wu, J.-T. Liu, K.-L. Zhang, W.-B. Chen, X.-Q. Song, J. W. Hair, and C.-Y. She, Appl. Opt. **41,** 7079 (2002).
7. J. Zhu, Y. Chen, Z. Yan, S. Wu, and Z. Liu, Chin. Opt. Lett. **6,** 449 (2008).
8. Z. S. Liu, B. Y. Liu, Z. G. Li, Z. A. Yan, S. H. Wu, and Z. B. Sun, Appl. Phys. B **88,** 327 (2007).
9. J. W. Müller, Nucl. Instrum. Methods **112,** 47 (1973).
10. D. N. Whiteman, Appl. Opt. **42,** 2571 (2003).
11. D. N. Whiteman, S. H. Melfi, and R. A. Ferrare, Appl. Opt. **31,** 3068 (1992).
12. M. S. Kang, D.-H. Lee, J. Lee, J. Y. Lee, S.-K. Choi, and H. S. Park, Metrologia **45,** 382 (2008).
13. D. N. Whiteman, B. Demoz, P. Di Girolamo, J. Comer, I. Veselovskii, K. Evans, Z. Wang, M. Cadirola, K. Rush, G. Schwemmer, B. Gentry, S. H. Melfi, B. Mielke, D. Venable, and T. Van Hove, J. Atm. Ocean. Technol. **23,** 157 (2006).